


FULL PAPER

Open Access



Temporal stability of coda Q in the northeastern part of an inland high strain rate zone, central Japan: implication of a persistent ductile deformation in the crust

Masanobu Dojo¹ and Yoshihiro Hiramatsu^{2*} 

Abstract

We have analyzed the temporal variation in coda Q in the northeastern part of an inland high strain rate zone, the Niigata–Kobe Tectonic Zone (NKTZ), in central Japan, to investigate the response of coda Q to the modification of the strain field induced by the 2011 Tohoku earthquake (Mw 9.0). We observe no statistically significant temporal variations in the spatial distribution of coda Q as the whole analyzed area, implying that the crustal deformation induced by the 2011 Tohoku earthquake has provided no significant temporal variation in crustal heterogeneity as the whole analyzed area. For the middle frequency bands, before and after the 2011 Tohoku earthquake, we have commonly found a negative correlation between the spatial distributions of coda Q and the differential strain rate and a positive correlation between the spatial distributions of coda Q and the perturbation of S-wave velocity in the upper crust. These features, together with previous works, suggest that the ductile deformation with a high rate in the upper crust plays an important role in generating the high strain rate in the analyzed area not only before but also after the 2011 Tohoku earthquake. In other words, the existence of a persistent ductile deformation in the upper crust contributes essentially to the generation process of the high strain rate in the northeastern part of the NKTZ. It is important to note that the location of the persistent ductile deformation in the northeastern part of the NKTZ, mainly in the upper crust, differs from that in the central part of the NKTZ, mainly in the lower crust.

Keywords: Niigata–Kobe Tectonic Zone, Heterogeneity, Aseismic deformation, The 2011 Tohoku earthquake

Introduction

Crustal stress and strain are fundamental factors to generate an inland earthquake. In recent decades, the progress in geodetic and seismological observations has revealed spatiotemporal variation in crustal activity, strain rate and seismicity, in detail. An inland high strain rate zone from Niigata to Kobe, called the Niigata–Kobe Tectonic Zone (NKTZ), in central Japan, revealed by a nation-wide dense GNSS observation network (Sagiya et al. 2000), is an important field in understanding the

generation process of inland earthquakes, in other words, the stress accumulation process to inland active faults.

Variation in stress and strain in the crust has also been clarified by the investigation of seismic waves. Coda Q and shear wave splitting as well as seismic velocity are sensitive to variation in crustal stress/strain. Okamoto et al. (2013) numerically analyzed the relationship between coda Q and stress. A spatial correspondence between a low coda Q area at lower frequency bands and the NKTZ was first pointed out by Jin and Aki (2005). This correspondence has been confirmed by Hiramatsu et al. (2010, 2013), Carcolé and Sato (2010), Tsuji et al. (2014) and Dojo and Hiramatsu (2017). Furthermore, Hiramatsu et al. (2010) reported that shear wave splitting and coda Q were a function of the strain rate in/around

*Correspondence: yoshizo@staff.kanazawa-u.ac.jp

² School of Geosciences and Civil Engineering, College of Science and Engineering, Kanazawa University, Kakuma, Kanazawa, Ishikawa 920-1192, Japan

Full list of author information is available at the end of the article

the NKTZ. They suggested that a high rate of ductile deformation below the brittle–ductile transition zone in the crust was a cause of the high strain rate in the NKTZ.

The 2011 off the Pacific coast of Tohoku earthquake (hereafter referred to as the 2011 Tohoku earthquake) caused large-scale coseismic and postseismic crustal deformations over the Japanese islands. These deformations have modified the crustal heterogeneities around the source area and caused a decrease of coda *Q* with center frequencies of 1.25–3.5 Hz along the Pacific coast of northeastern Japan (Padhy et al. 2013).

Recently, Meneses-Gutierrez and Sagiya (2016) have investigated a temporal change in E–W contraction of strain rate in the northeastern part of the NKTZ between before and after the 2011 Tohoku earthquake. They showed that a short-wavelength component of E–W contraction was maintained, in spite of a large elastic response due to the 2011 Tohoku earthquake, and concluded that a persistent localized contraction was caused by a shallow aseismic slip from the lower crust to a part of the upper crust, driven by the absolute stress.

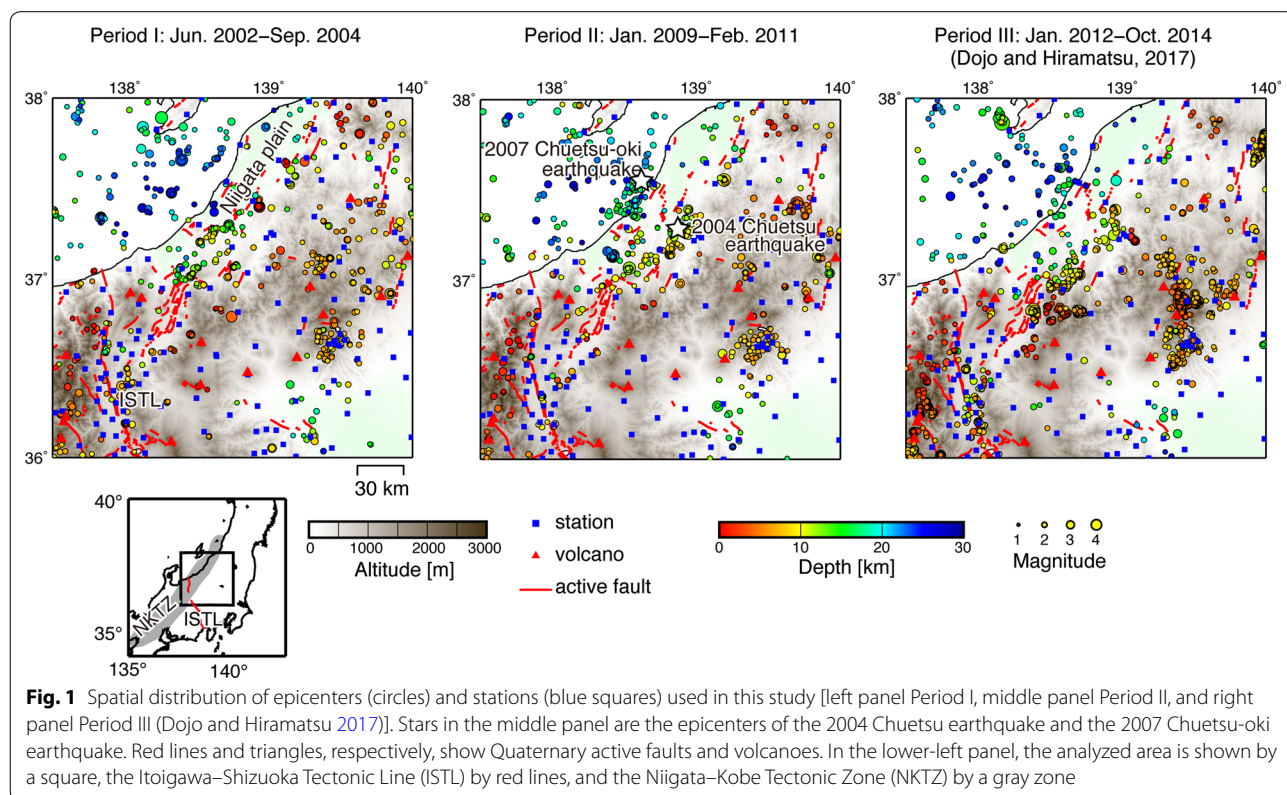
Dojo and Hiramatsu (2017) investigated a spatial variation in coda *Q* in the northeastern part of the NKTZ (NE-NKTZ). Based on correlations between the spatial distribution of coda *Q*, the perturbation of S-wave velocity (Nakajima and Hasegawa 2007), and the strain rate,

they suggested that a high rate of ductile deformation in the upper crust might play an important role to generate a high strain rate in the NE-NKTZ. However, their analysis was limited after the 2011 Tohoku earthquake and it has been unclear whether the spatial distribution of coda *Q* is temporally stable or not in the NE-NKTZ. The temporal stability of coda *Q* would provide another piece of evidence of the persistent ductile deformation in the crust in the NE-NKTZ.

This present study focuses on the temporal variation in coda *Q* before and after the 2011 Tohoku earthquake. We demonstrate that coda *Q* shows no significant temporal variation as the whole area of the NE-NKTZ. From this temporal variation and geodetic observations reported previously, we conclude that a high deformation rate zone in the ductile part in the upper crust may have been persistently present in the NE-NKTZ.

Data and method

The analyzed area is the NE-NKTZ, where Dojo and Hiramatsu (2017) reported the detailed spatial distribution of coda *Q* after the 2011 Tohoku earthquake (Fig. 1). The period for the investigation of coda *Q* is June 2002–February 2011. The values of coda *Q* would vary after a large earthquake around the source region (e.g., Hiramatsu et al. 2000), and a few years



are needed to recover the crustal condition prior to the earthquake (Sugaya et al. 2009). There are two large earthquakes between June 2002–February 2011 in the analyzed area; the 2004 Chuetsu earthquake (October 23, 2004; M_{JMA} 6.8) and the 2007 Chuetsu-Oki earthquake (July 16, 2007; M_{JMA} 6.8). Therefore, we excluded the periods immediately after these earthquakes and set the analysis periods from June 2002–September 2004 (period I) and from January 2009–February 2011 (period II).

The criteria for the selection of events are identical to those of Dojo and Hiramatsu (2017), that is, magnitudes greater than 1.8, focal depths shallower than 30 km, and epicentral distances at each station less than 30 km. For the data after the 2011 Tohoku earthquake (period III: January 2012–October 2014), we used the results reported by Dojo and Hiramatsu (2017). Seismic waveforms used in this study are recorded at stations of the Earthquake Research Institute, University of Tokyo; the Disaster Prevention Research Institute, Kyoto University; the Research Center for Prediction of Earthquakes and Volcanic Eruptions, Tohoku University; the Japan Meteorological Agency; and Hi-net data operated by National Research Institute for Earth Science and Disaster Resilience, which are the same as those used by Dojo and Hiramatsu (2017). We have analyzed 672 events in the period I and 646 events in the period II in this study (Fig. 1).

For the analysis of coda Q (Q_C), we applied the single back scattering model (Aki and Chouet 1975), $\ln A_C(f|t) = -\ln t - \pi f Q_C^{-1} t + \text{const}$, where $A_C(f|t)$ is the RMS amplitude of the band-pass filtered coda wave at the center frequency f and the lapse time t , and followed the procedure of Dojo and Hiramatsu (2017) (see the details in Dojo and Hiramatsu (2017)). We calculated the root mean square (RMS) amplitude of velocity waveform of each component for five frequency bands, 1–2, 2–4, 4–8, 8–16, and 16–32 Hz. The time window for the fitting of the single back scattering model is from the twice the arrival time of the S-wave to the time when the RMS amplitude is equal to twice the noise level. If this end time is greater than 30 s after the origin time, we set the end time to be 30 s, to avoid the effect of multiple scattering. The lapse time of 30 s corresponds to the farthest scatters from the station, located at 45 km (Jin and Aki 2005). If the end time is shorter than 5 s, we exclude the data. For each event, we calculated the average value of $\log_{10} Q_C^{-1}$ of three components at each station for each band. An example of the estimation of coda Q is shown in Fig. 2.

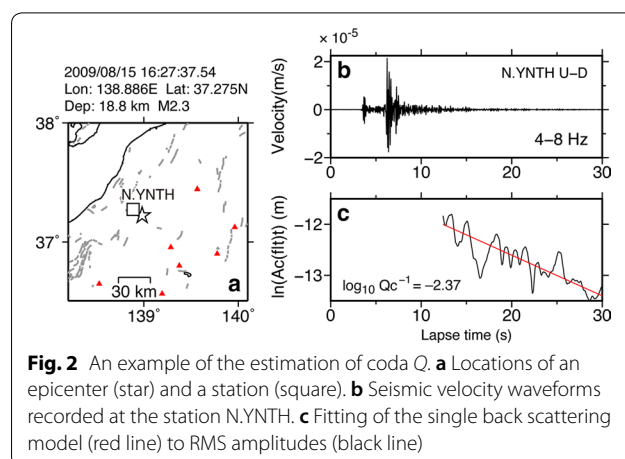


Fig. 2 An example of the estimation of coda Q . **a** Locations of an epicenter (star) and a station (square). **b** Seismic velocity waveforms recorded at the station N.YNTH. **c** Fitting of the single back scattering model (red line) to RMS amplitudes (black line)

Results

Spatial distribution of coda Q

The spatial distributions of coda Q in the periods I and II, together with that in the period III reported by Dojo and Hiramatsu (2017), are shown in Fig. 3. For each band, we used stations at which the value of coda Q is obtained for more than 5 events. We made the map of the spatial distribution of coda Q with spatial smoothing of every 10 min at longitude and latitude by using the surface command of GMT (Wessel and Smith 1998).

The spatial distributions of coda Q seem to be similar between the periods I and II, although we obtain a relatively poor distribution of coda Q in the period I. In the low frequency bands (1–2 and 2–4 Hz), low coda Q is distributed around the Itoigawa–Shizuoka Tectonic Line (ISTL) and some volcanoes and high coda Q around the Niigata plain. In the middle frequency bands (4–8 and 8–16 Hz), low coda Q is distributed from the southwestern Niigata plain to ISTL and high coda Q in other areas such as north Kanto district. These distributions in the lower and middle frequency bands are coincident with those of Carcolé and Sato (2010). On the other hand, it is difficult to observe a distinct spatial distribution of coda Q in the high frequency band (16–32 Hz). These features of the spatial distributions of coda Q in the periods I and II are similar to those in the period III reported by Dojo and Hiramatsu (2017).

Temporal variation in coda Q

To examine a temporal variation in coda Q , we focused on stations at which we obtain the value of coda Q for more than 10 events for each band in each period. In each period, we calculated the mean and standard deviation of $\log_{10} Q_C^{-1}$, and also the difference of the mean of

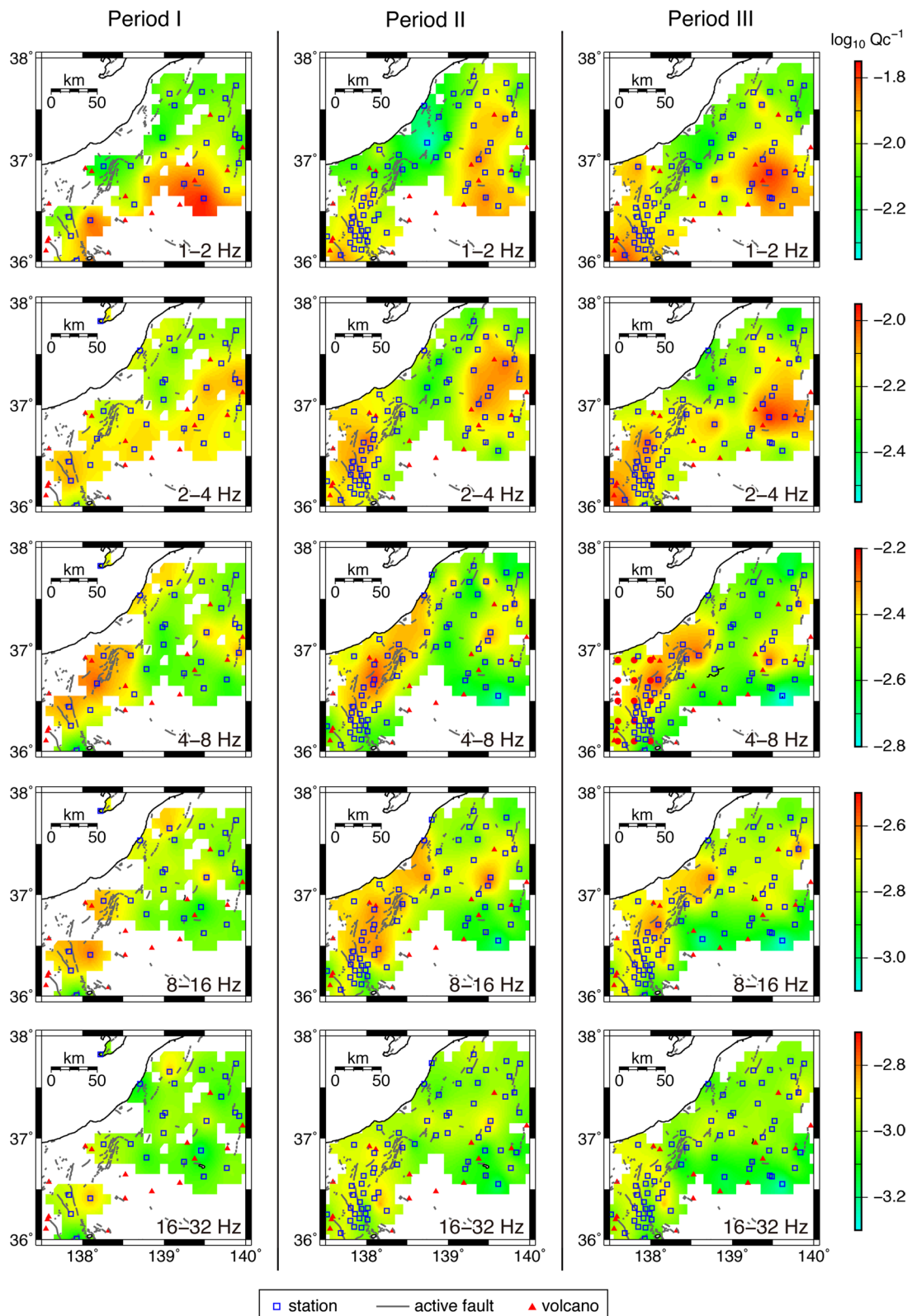


Fig. 3 Spatial distributions of coda Q^{-1} at five frequency bands in the Period I (left panels), the Period II (middle panels), and the Period III (right panels; Dojo and Hiramatsu 2017). Blue squares are stations used to draw the coda Q maps. Gray lines show Quaternary active faults, and red triangles show Quaternary active volcanoes

the $\log_{10} Q_C^{-1}$ for the two successive periods. To evaluate the statistical significance of the differences, we applied the Welch's t test. Here the null hypothesis is that the true difference in means is equal to 0. If we choose the threshold for statistical significance as 0.05, then a p value less than 0.05 rejects the null hypothesis. This is interpreted that the difference in means is statistically significant.

Figure 4 shows an example of the temporal variation in coda Q at 4–8 Hz band, together with the mean value and the standard deviation, in each period at the station N.YNTH. This shows no significant variations and large p values for the differences of the mean between the periods I and II and between the periods II and III, although there are scattered data. Figure 5 shows the spatial distribution of the difference of the mean of $\log_{10} Q_C^{-1}$ for the two successive periods, subtracting the preceding ones from the subsequent ones. Most of the differences are within ± 0.2 for all frequency bands. The standard deviations of $\log_{10} Q_C^{-1}$ are generally ~ 0.2 , meaning that most of the differences are within the standard deviations. The results of the Welch's t test show that most of the stations have a large p value, greater than 0.05 (Fig. 6), indicating that the difference of the mean value of the two successive periods is not statistically significant. On the other hand, there are some stations with small p values for each band between the periods II and III. However, these stations are rather distributed in isolation in the analyzed region. In other words, the temporal variations at these stations might reflect the modification of crustal heterogeneity not over the whole analyzed region but in the vicinity of the stations. In fact, we can observe the increase of seismicity around some of these stations (Fig. 1), suggesting a local variation in stress/stressing rate. Therefore, we conclude that the spatial distribution of coda Q shows no statistically significant temporal variation as the whole analyzed region in the NE-NKTZ throughout the analyzed periods.

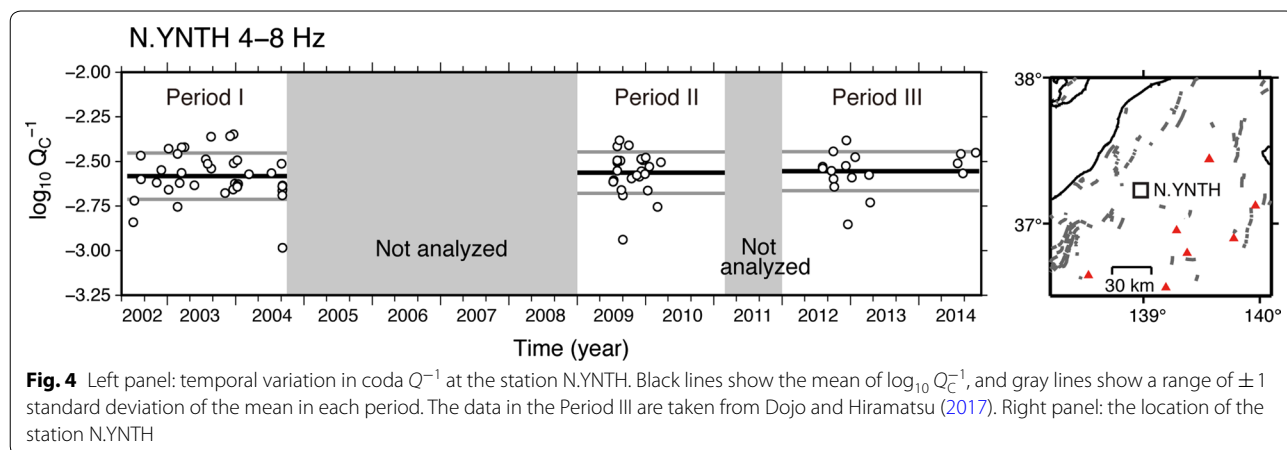
As we mentioned in Introduction, Padhy et al. (2013) found a decrease of coda Q with center frequencies of 1.25–3.5 Hz near the source area of the 2011 Tohoku earthquake. The main difference between this study and Padhy et al. (2013) is the distance between the analyzed area and the source area of the 2011 Tohoku earthquake. The analyzed area of this study is far from the source area, causing not only a relatively smaller magnitude of the variation in strain/stress and those rates but also a relatively longer wavelength of the variation. We suggest that both the smaller magnitude and the longer wavelength of the variation could not modify effectively the heterogeneity in the crust, because coda Q is sensitive not only to the magnitude but also the variation of the rates (Hiramatsu et al. 2013).

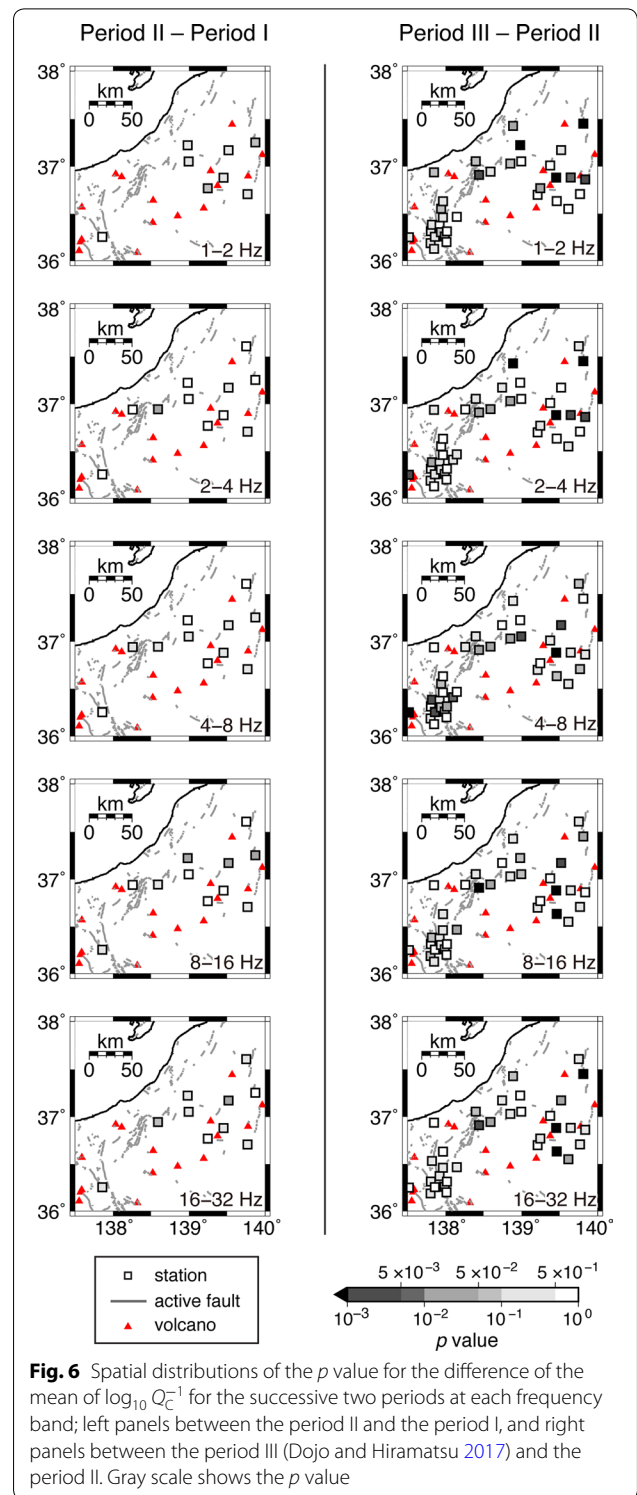
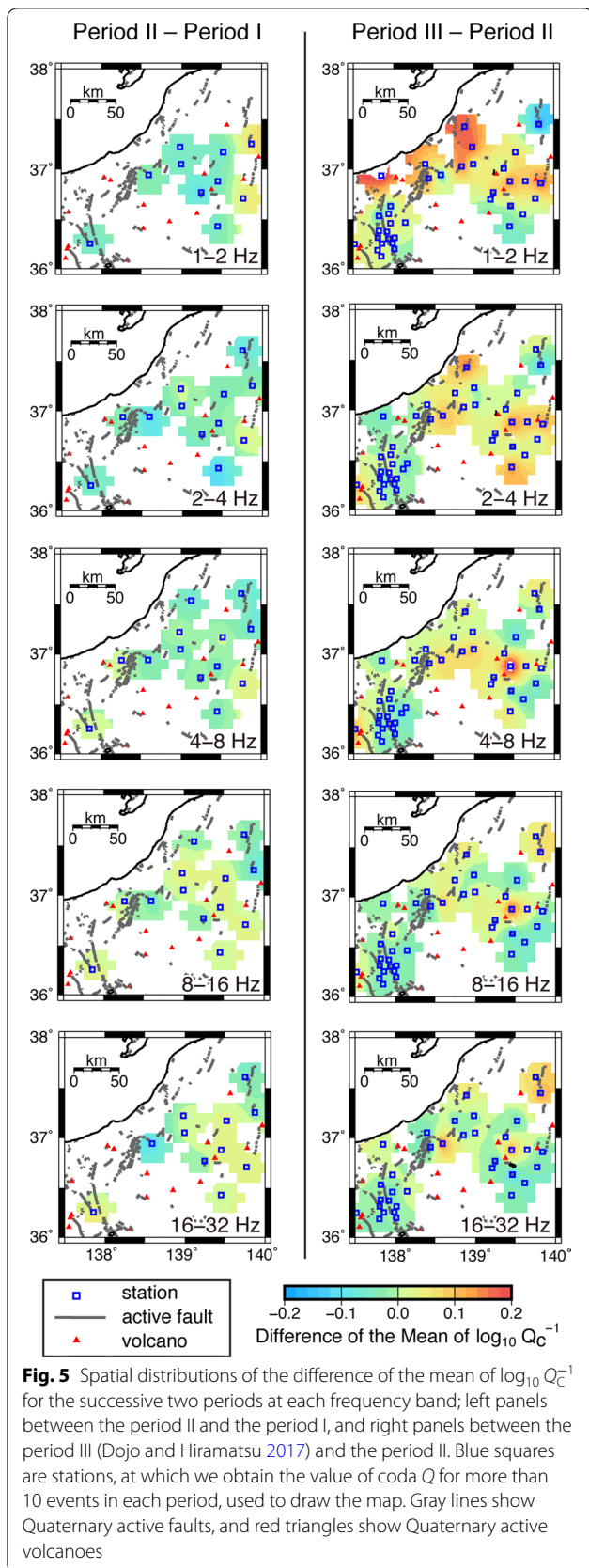
Discussion

Relationships between coda Q , differential strain rate and S-wave velocity

As presented by Dojo and Hiramatsu (2017), we compare the spatial distributions of coda Q in the periods I and II to the differential strain rate estimated from GNSS data in the same periods, June 2002–September 2004 and January 2009–February 2011 (Fig. 7) and the perturbations of S-wave velocity (Nakajima and Hasegawa 2007). The differential strain rate is calculated by subtracting the value of the principal strain rate of the compression axis from that of the extension axis, which is twice that of the shear strain rate.

For the comparison, we combine the data of coda Q in the periods I and II, because the number of data in the period I is small and the temporal variation in coda Q between the periods I and II is not statistically significant. Furthermore, as shown in Fig. 7, the spatial distribution in the differential strain rate is almost the same between the periods I and II, before the 2011 Tohoku earthquake. We sample the values of coda Q in each frequency band,





the differential strain rates and the perturbation of the S-wave velocity at each depth at $0.2^\circ \times 0.2^\circ$ and calculate the correlation coefficient and p value between the two quantities.

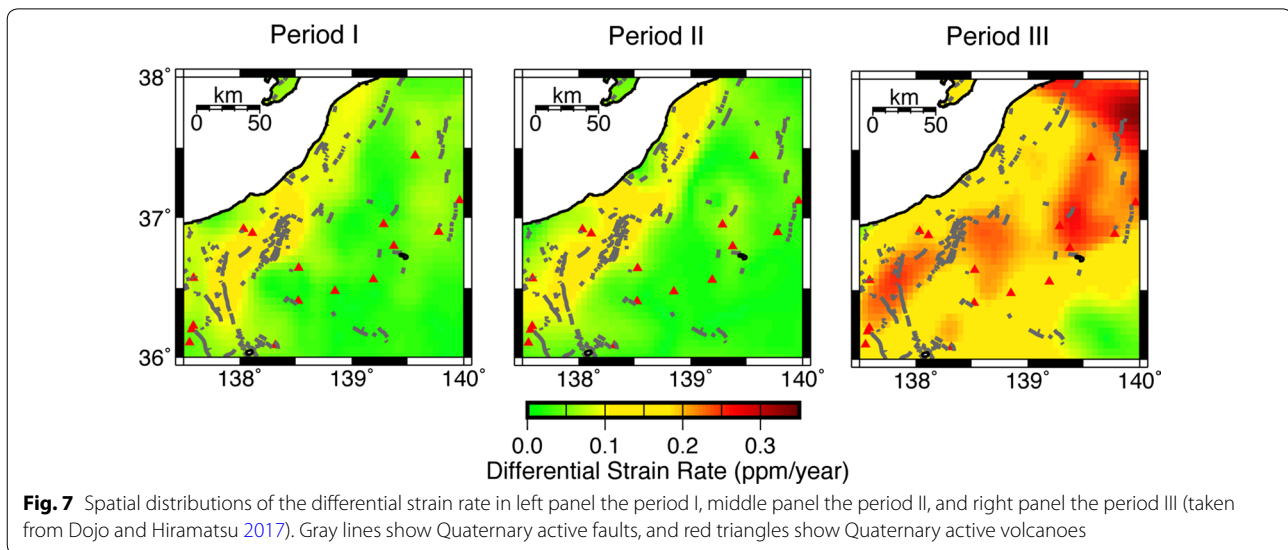


Figure 8 shows that we recognize negative correlations between the coda Q and the differential strain rate in the middle (4–8 and 8–16 Hz) and the highest frequency (16–32 Hz) bands and a positive correlation in the lowest frequency (1–2 Hz) band. These correlations are observed commonly in spite of the selection of the strain rate data between the periods I and II. However, it is difficult to find a negative correlation for the 2–4 Hz frequency band, which was recognized in the result of Dojo and Hiramatsu (2017).

It is interesting that the correlations between coda Q and the strain rate in all the frequency bands except for the 2–4 Hz frequency band observed in the periods I and II is clearer than those in the period III (Dojo and Hiramatsu 2017). This might result from the modification of the strain rate field caused by coseismic and postseismic deformation of the 2011 Tohoku earthquake, which makes the correlations lower. In other words, we can consider that the correlations before the 2011 Tohoku earthquake reflect more directly the features of the NKTZ because of no modification of the strain field induced by the 2011 Tohoku earthquake. The negative correlation for the 2–4 Hz frequency band after the 2011 Tohoku earthquake (Dojo and Hiramatsu 2017) is likely to be affected by the modification of the strain field. The positive correlation observed for the lowest frequency band is likely to be a result of the soft layer as discussed by Dojo and Hiramatsu (2017).

Figure 8 also shows a sensitivity of coda Q to the differential strain rate. We focus here the frequency bands of 4–8, 8–16, and 16–32 Hz, which show a negative correlation with statistical significance between the differential strain rate and coda Q . The least squares fit of each

plot, respectively, provides the slope of -1216 ± 179 , -1651 ± 315 , and -1351 ± 455 at 4–8, 8–16, and 16–32 Hz frequency bands for the differential strain rate in the Period I, and those of -1118 ± 150 , -1659 ± 255 and -1561 ± 377 at 4–8, 8–16, and 16–32 Hz frequency bands for the differential strain rate in the Period II. These values also, respectively, lead the fractional change of coda Q , defined as $\Delta Q_C/Q_C$ (Fig. 8), of 0.42, 0.31, and 0.16 at 4–8, 8–16, and 16–32 Hz frequency bands for the differential strain rate in the Period I, and those of 0.39, 0.32, and 0.18 at 4–8, 8–16, and 16–32 Hz frequency bands for the differential strain rate in the Period II. The values of $\Delta Q_C/Q_C$ at the middle frequency band are comparable to those at the lower frequency bands (0.31 at 1.5 Hz and 0.38 at 2 Hz) around the Atotsugawa fault zone (Hiramatsu et al. 2013).

In the upper crustal depths, the correlations between coda Q and the perturbations of S-wave velocity are positive and statistically significant for the middle frequency bands (4–8 and 8–16 Hz) in this study (Fig. 9). Hiramatsu et al. (2013) reported the positive correlations between those at the lower frequency bands around the Atotsugawa fault zone located in the central part of the NKTZ. We suggest that this difference might reflect the difference in the dominant fracture size of ductile deformation at different depths between the two areas. For the lower frequency bands (1–2 and 2–4 Hz), negative correlations with statistical significance are found at the depths shallower than 5 km, while no statistically significant correlations are found at a 10 km depth. On the other hand, in the lower crustal depths, the correlations are positive and statistically significant for the lower frequency bands

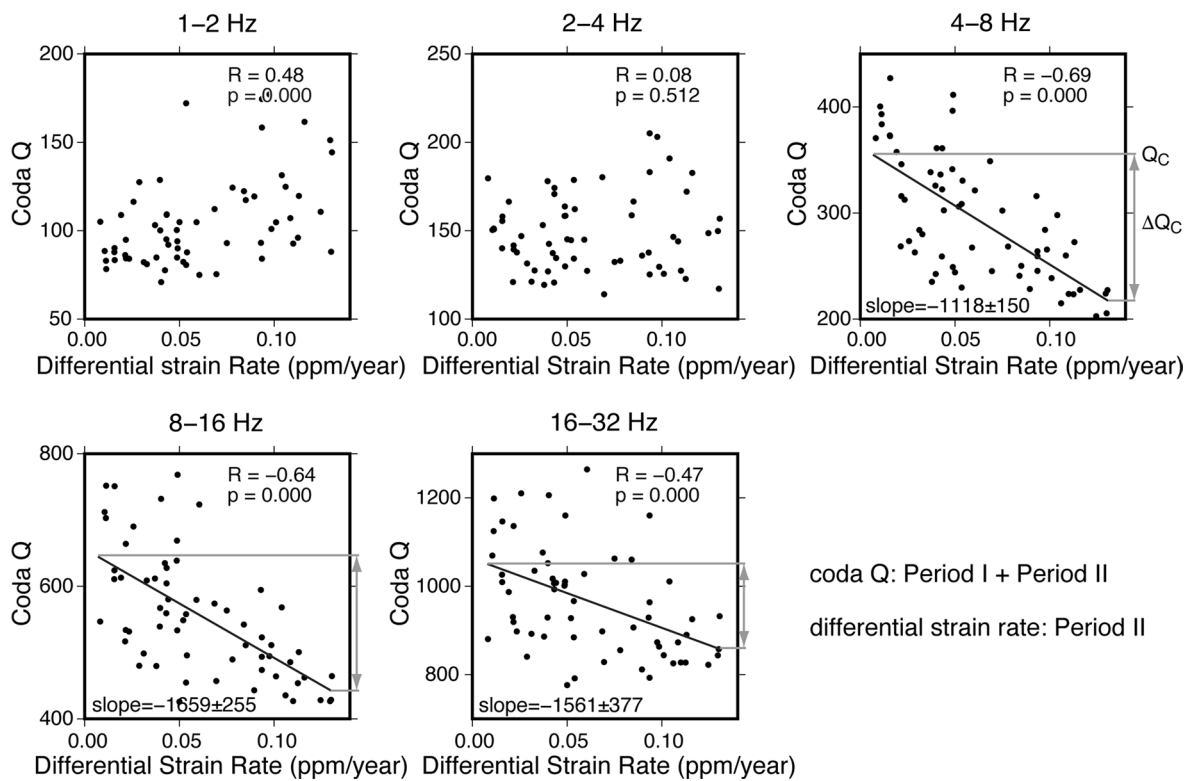
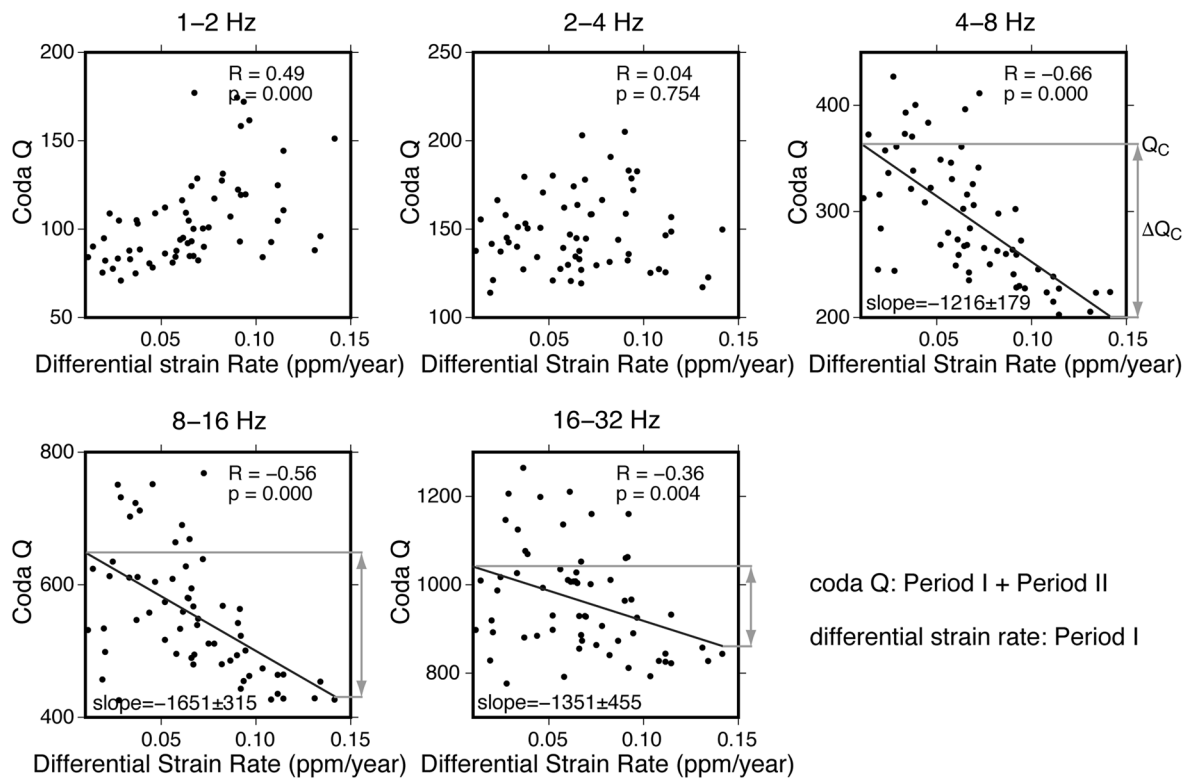
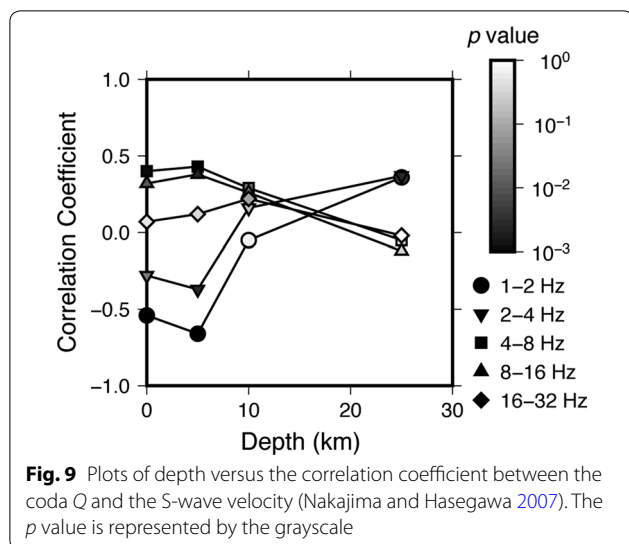


Fig. 8 Upper panels: plots of differential strain rate in the period I versus coda Q at five frequency bands in the periods I and II. Lower panels: plots of differential strain rate in the period II versus coda Q at five frequency bands in the periods I and II. Black line is the least square fit to the plot. Gray lines represent the definition of ΔQ_C and Q_C



at a 25 km depth. These features are similar to those of Dojo and Hiramatsu (2017).

Implication for persistent ductile deformation in the crust

As we described in "Temporal variation in coda Q " section, the coda Q in the NE-KETZ shows no statistically significant temporal variation as a whole region. We discuss here what this result, together with the relationships we mentioned in the previous subsection, implies.

Hiramatsu et al. (2013) emphasized two correlations, a negative correlation between coda Q and the differential strain rate and a positive correlation between coda Q and the perturbation of S-wave velocity, as indicators of ductile deformation with a high rate in the crust. In terms of this kind of view, as we describe in the previous section, both correlations are confirmed only at the middle frequency band (4–8 Hz) through the periods I–III in this study. The same correlations are also found even in 8–16 frequency bands in the periods I and II. These correlations suggest that the ductile deformation in the upper crust has played an important role to generate the high strain rate in the NE-NKTZ not only before but also after the 2011 Tohoku earthquake. In other words, the existence of the correlations all throughout the periods suggests the existence of the persistent ductile deformation with higher deformation rate than the surrounding region, that is, persistent aseismic deformation.

This is coincident with the temporal variation in the short-wavelength strain rate, which corresponds to the width of the NE-NKTZ, observed by GNSS (Meneses-Gutierrez and Sagiya 2016). Meneses-Gutierrez and Sagiya (2016) showed no significant temporal variation in the short-wavelength strain rate before and after the 2011 Tohoku earthquake and attributed the cause to aseismic fault movement from the lower to the middle of the

upper crust. They stressed that it is important that the aseismic fault movement would be persistent beneath the NE-NKTZ before and after the 2011 Tohoku earthquake.

Recently, before and after the 2011 Tohoku earthquake, a similar spatial pattern of the strain rate with short wavelength has been confirmed around the Atotsugawa fault zone (Inamatsu et al. 2017), in the center of the high strain rate zone. From the correlations between coda Q , the differential strain rate and the S-wave velocity around the Atotsugawa fault zone, Hiramatsu et al. (2013) suggested that a high rate of the ductile deformation below the brittle–ductile transition zone in the crust was likely to cause the high strain rate zone on the ground surface. The result of Inamatsu et al. (2017) can be interpreted as the existence of the persistent aseismic deformation beneath the Atotsugawa fault zone.

There is additional research for temporal variation in coda Q in the high strain rate zone before and after the 2011 Tohoku earthquake. Tsuji et al. (2014) reported no statistically significant temporal variation in coda Q in/around the source region of the 1891 Nobi earthquake, in the central part of NKTZ. This observation would support the idea of the existence of the persistent ductile deformation in the crust as a cause of the high strain rate zone in/around the source region of the 1891 Nobi earthquake.

It is important to note the difference in the location of the persistent ductile deformation in the NKTZ as the cause of the high strain rate zone suggested by coda Q analyses; in the upper crust in the NE-NKTZ and in the lower crust in the central NKTZ. The difference in depth of the elastically weakened part of the NKTZ revealed by Nakajima and Matsuzawa (2017) supports the heterogeneous depth distribution of the persistent ductile deformation in the NKTZ.

Conclusions

The spatial distribution of coda Q in the northeastern part of NKTZ before the 2011 Tohoku earthquake is examined to investigate a temporal stability of the distribution of coda Q . We also use the result of our previous work to compare the distribution of coda Q before and after the 2011 Tohoku earthquake. We reveal that the spatial distribution of coda Q has not been modified as the whole analyzed area, regardless of the strain rate change caused by the 2011 Tohoku earthquake. We also confirm that the spatial distributions of coda Q in the middle frequency bands are correlated negatively with the differential strain rate and positively with the perturbation of S-wave velocity in the upper crust. In 4–8 Hz frequency band, those correlations are confirmed for all through the analyzed periods, that is, in both the periods before and after the 2011 Tohoku earthquake, suggesting

a persistent cause of the correlations independent of the modification of the strain rate due to the 2011 Tohoku earthquake. The correlations observed in this study, together with previous works, would lead to the conclusion that the existence of persistent ductile deformation with a high rate is likely to be a main cause to generate the inland high strain rate zone in the NKTZ. However, the difference of the correlations, as well as the velocity structures between the northeastern and the central NKTZ, suggests that a difference in the location of the persistent ductile deformation: mainly in the upper crust in the northeastern part and in the lower crust in the central part of the NKTZ.

Abbreviations

NKTZ: Niigata–Kobe Tectonic Zone; NE-NKTZ: Northeastern part of the Niigata–Kobe Tectonic Zone; ISTL: Itoigawa–Shizuoka Tectonic Line; GMT: general mapping tools; GNSS: global navigation satellite system.

Authors' contributions

YH designed this study. MD and YH conducted the analyses and drafted the manuscript. Both authors read and approved the final manuscript.

Author details

¹ Graduate School of Natural Science and Technology, Kanazawa University, Kakuma, Kanazawa, Ishikawa 920-1192, Japan. ² School of Geosciences and Civil Engineering, College of Science and Engineering, Kanazawa University, Kakuma, Kanazawa, Ishikawa 920-1192, Japan.

Acknowledgements

We thank the National Research Institute for Earth Science and Disaster Resilience, the Japan Meteorological Agency, Tokyo University, Kyoto University, and Tohoku University for allowing us to use waveform data collected at each online station. We are grateful to Junichi Nakajima and Takuya Nishimura for providing us with seismic tomography data and with strain rate data, respectively. The constructive comments of anonymous reviewers, Toru Matsuzawa, and Carsten Booth were also helpful to improve the manuscript. All figures were made using GMT software (Wessel and Smith 1998).

Competing interests

The authors declare that they have no competing interests.

Availability of data and materials

The waveform data of the Hi-net stations and the other institutes are available from the NIED web site (<http://www.bosai.go.jp>).

Funding

This study is supported by JSPS KAKENHI Grant Number 261090003.

Publisher's Note

Springer Nature remains neutral with regard to jurisdictional claims in published maps and institutional affiliations.

Received: 17 December 2018 Accepted: 9 March 2019

Published online: 15 March 2019

References

- Aki K, Chouet B (1975) Origin of coda waves: source, attenuation and scattering effects. *J Geophys Res* 80:3322–3342
- Carcolé E, Sato H (2010) Spatial distribution of scattering loss and intrinsic absorption of short-period *S* waves in the lithosphere of Japan on the basis of the multiple lapse time window analysis of Hi-net data. *Geophys J Int* 180:268–290
- Dojo M, Hiramatsu Y (2017) Spatial variation in coda *Q* in the northeastern part of Niigata–Kobe tectonic zone, central Japan: implication of the cause of a high strain rate zone. *Earth Planets Space* 69:76. <https://doi.org/10.1186/s40623-017-0663-x>
- Hiramatsu Y, Hayashi N, Furumoto M, Katao H (2000) Temporal changes in coda Q^{-1} and *b*-value due to the static stress change associated with the 1995 Hyogo-ken Nanbu earthquake. *J Geophys Res* 105:6141–6151
- Hiramatsu Y, Iwatsuki K, Ueyama S, Iidaka T, The Japanese University Group of the Joint Seismic Observations at NKTZ (2010) Spatial variation in shear wave splitting of the upper crust in the zone of inland high strain rate, central Japan. *Earth Planets Space* 62:675–684. <https://doi.org/10.5047/eps.2010.08.003>
- Hiramatsu Y, Sawada A, Yamauchi Y, Ueyama S, Nishigami K, Kurashimo E, The Japanese University Group of the Joint Seismic Observations at NKTZ (2013) Spatial variation in coda *Q* and stressing rate around the Atotsugawa fault zone in a high strain rate zone, central Japan. *Earth Planets Space* 65:115–119. <https://doi.org/10.5047/eps.2012.08.012>
- Inamatsu T, Takada Y, Sagiya T, Nishimura T (2017) Crustal deformation in and around the Atotsugawa fault before and after the Tohoku-Oki earthquake. Abstracts of IAG-IASPEI J05-5-03
- Jin A, Aki K (2005) High-resolution maps of coda *Q* in Japan and their interpretation by the brittle–ductile interaction hypothesis. *Earth Planets Space* 57:403–409. <https://doi.org/10.1186/BF03351825>
- Meneses-Gutierrez A, Sagiya T (2016) Persistent inelastic deformation in central Japan revealed by GPS observation before and after the Tohoku-oki earthquake. *Earth Planet Sci Lett* 450:366–371. <https://doi.org/10.1016/j.epsl.2016.06.055>
- Nakajima J, Hasegawa A (2007) Deep crustal structure along the Niigata–Kobe Tectonic Zone, Japan: its origin and segmentation. *Earth Planets Space* 59:e5–e8. <https://doi.org/10.1186/BF03352677>
- Nakajima J, Matsuzawa T (2017) Anelastic properties beneath the Niigata–Kobe Tectonic Zone, Japan. *Earth Planets Space* 69:33. <https://doi.org/10.1186/s40623-017-0619-1>
- Okamoto K, Mikada H, Goto T, Takekawa J (2013) Numerical analysis of the relationship between time-variant coda-*Q* and the variation in crustal stress. *Geophys J Int* 195:575–581
- Padhy S, Takemura S, Takemoto T, Maeda T, Furumura T (2013) Spatial and temporal variation in coda attenuation associated with the 2011 off the Pacific coast of Tohoku, Japan (Mw 9) earthquake. *Bull Seismol Soc Am* 103:1411–1428
- Sagiya T, Miyazaki S, Tada T (2000) Continuous GPS array and present-day crustal deformation of Japan. *PAGEOPH* 157:2003–2322
- Sugaya K, Hiramatsu Y, Furumoto M, Katao H (2009) Coseismic change and recovery of scattering environment in the crust after the 1995 Hyogo-ken Nanbu earthquake, Japan. *Bull Seismol Soc Am* 99:435–440
- Tsuji S, Hiramatsu Y, The Japanese University Group of the Joint Seismic Observations at the Area of Nobi Earthquake (2014) Spatial variation in coda *Q* around the Nobi fault zone, central Japan: relation to *S*-wave velocity and seismicity. *Earth Planets Space* 66:97. <https://doi.org/10.1186/1880-5981-66-97>
- Wessel P, Smith WHF (1998) New, improved version of generic mapping tools released. *EOS Trans Am Geophys Union* 79:579